Classical treatment of parametric processes in a strong-coupling planar microcavity

D. M. Whittaker
Toshiba Research Europe Limited, 260 Cambridge Science Park, Cambridge CB4 OWE, United Kingdom
(Received 21 January 2001; published 27 April 2001)

A classical treatment of parametric scattering in strong-coupling semiconductor microcavities is shown to provide a good description of recent experiments in which parametric oscillator behavior has been demonstrated. The model consists of a nonlinear excitonic oscillator coupled to a cavity mode that is driven by the external fields and predicts the output power, below threshold gain and spectral blueshifts of the parametric oscillator.

DOI: 10.1103/PhysRevB.63.193305 PACS number(s): 42.65.Yj, 71.36.+c, 78.20.Bh

Recent experimental studies have demonstrated that very large optical nonlinearities can be obtained in resonantly pumped strong-coupling microcavities. The excitations of these structures are polaritons, mixed modes that are part exciton and part cavity photon, and the nonlinearity is due to interactions between the exciton components that cause the polaritons to scatter off each other. This leads to a parametric process where a pair of pump polaritons scatter into nondegenerate signal and idler modes while conserving energy and momentum. The scattering is particularly strong in microcavities because the unusual shape of the dispersion, shown in the inset to Fig. 1, makes it possible for pump, signal, and idler all to be on resonance at the same time.

A further important property of planar microcavities is the correspondence between the in-plane momentum of each polariton mode and the direction of the external photon to which it couples. This makes it quite straightforward to investigate parametric scattering using measurements at different angles to access the various modes. Two types of processes have been studied in this way: parametric amplification, where the scattering is stimulated by excitation of the signal mode with a weak probe field, and parametric oscillation, where there is no probe and a coherent population in the signal mode appears spontaneously.

Parametric amplification in microcavities was first observed by Savvidis *et al.*,[1] using ultrafast pump-probe measurements. The structure was pumped on the lower polariton branch at an incident angle of 16.5°. Narrow band gains of up to 70 were observed in the region of the polariton feature for a probe at 0°, along with idler emission at 35°. These are a set of angles for which the pair scattering resonance condition is satisfied. A related scattering process has been studied by Huang *et al.*[2] using two pump beams at ±45° and a probe at normal incidence. The experimental results of Ref. 1 have been modeled by Ciuti *et al.*[3] using a microscopic quantum treatment of polariton-polariton interactions.

Parametric oscillator behavior has been observed by Stevenson *et al.*[4] and Baumberg *et al.*,[5] in cw experiments with the pump incident on the lower polariton branch at the ''magic'' angle of about 16°. Above a threshold pump intensity, strong signal and idler beams were observed at about 0° and 35°, without any probe stimulation. The coherence of these beams was demonstrated by significant spectral narrowing, proving that they are due to a parametric process rather than resonantly enhanced incoherent photoluminescence. Houdré *et al.*,[6] have also observed a nonlinear emission at 0° for a structure pumped at 10°. However, in this experiment the pair scattering resonance condition is not satisfied, suggesting that different physics may be involved.

The purpose of this paper is to develop a simple classical model which provides a unified treatment of both amplifier and oscillator in the cw regime. This model is based on the textbook treatment of parametric phenomena in systems such as $LiNbO_3$.[7] Indeed, the microcavity behavior has characteristics similar to a typical doubly resonant parametric oscillator, where just the signal and idler modes are cavity resonances—the pump resonance is mainly important in enhancing the strength of the nonlinear effects. However, there are also significant novel aspects to the model: the microcavity operates in the strong-coupling regime, where the modes are cavity polaritons not simple photons, and instead of a non-resonant $\chi^{(2)}$ nonlinearity, the exciton provides a highly resonant $\chi^{(3)}$ effect.

I. MODEL

The theoretical model is a classical treatment of a nondispersive exciton mode $\psi(r)$ with energy ω_x coupled to a cavity mode $\phi(r)$ with dispersion $\omega_c(k)$, which is driven by the external fields. To account for broadening processes, ω_x and $\omega_c(k)$ are taken to be complex energies with imaginary parts γ_x and γ_c, respectively. The exciton mode is nonlinear, with potential energy $V(\psi)=\frac{1}{2}\omega_x^2\psi^2+\frac{1}{12}\kappa\psi^4$.

To model the parametric processes, the cavity is driven by harmonic plane waves, consisting of a pump with amplitude F_p at $(\omega_p,\mathbf{k}_p)$ and a probe with amplitude F_s at $(\omega_s,\mathbf{k}_s)$. The cavity and exciton modes are also expressed as a sum of plane waves at $(\omega_p,\mathbf{k}_p)$ and $(\omega_s,\mathbf{k}_s)$, plus an idler at $(\omega_i=2\omega_p-\omega_s,\mathbf{k}_i=2\mathbf{k}_p-\mathbf{k}_s)$. The cavity mode is linear, so the equations of motion for the pump, signal, and idler mode separate out, giving

$$\begin{aligned}[\omega_c(k_p)^2-\omega_p^2]\phi_p+g\psi_p&=F_p,\\ [\omega_c(k_s)^2-\omega_s^2]\phi_s+g\psi_s&=F_s,\\ [\omega_c(k_i)^2-\omega_i^2]\phi_i+g\psi_i&=0,\end{aligned}\tag{1}$$

where g is the strength of the coupling between the exciton and the cavity photon. The exciton equations are more complicated because the nonlinearity generates many terms at different frequencies and wave vectors. Only the terms at frequencies ω_p, ω_s, ω_i are retained here: the others are at very different frequencies, such as $3\omega_p$, or are weak, less than $O(\psi_p^2)$. This leaves

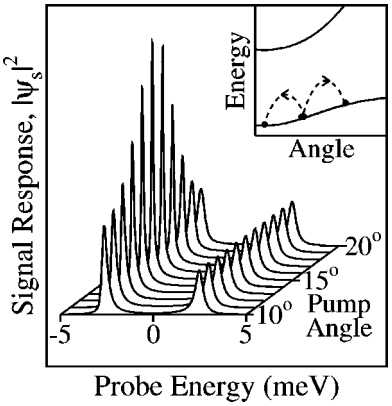

FIG. 1. Dependence of the signal response on the pump angle, with a probe at normal incidence. The pump amplitude $f_p=0.292$, which corresponds to $I_p=0.75I_0$ for this geometry. Structure parameters are Rabi splitting $\Omega=5.0$ meV, zero detuning, exciton width $\gamma_x=0.25$ meV, cavity width $\gamma_c=0.25$ meV, nonlinearity $\bar{\kappa}=1$. The inset shows the polariton dispersion with the pair scattering from pump to signal and idler modes.

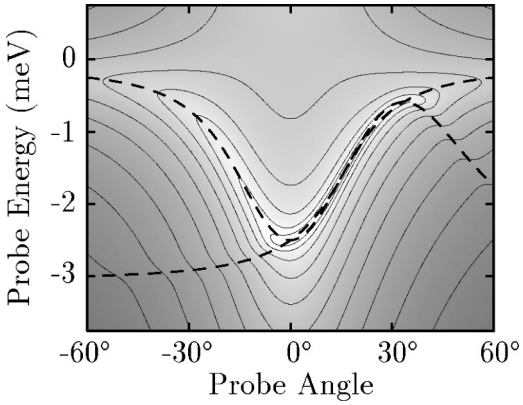

FIG. 2. Contour plot of the signal response $|\psi_s|^2$ as a function of probe energy and incidence angle. The contours are logarithmically spaced, and the light regions of background shading indicate the highest intensities. Dashed lines show the single resonance conditions for the signal and idler. The pump is on resonance at 16°, and other parameters are as in Fig. 1.

$$
\begin{aligned}
&(\omega_x^2-\omega_p^2)\psi_p+g\phi_p+\kappa|\psi_p|^2\psi_p+2\kappa\psi_s\psi_i\psi_p^*=0,\\
&(\omega_x^2-\omega_s^2)\psi_s+g\phi_s+2\kappa|\psi_p|^2\psi_s+\kappa\psi_p^2\psi_i^*=0, \qquad (2)\\
&(\omega_x^2-\omega_i^2)\psi_i+g\phi_i+2\kappa|\psi_p|^2\psi_i+\kappa\psi_p^2\psi_s^*=0.
\end{aligned}
$$

These equations can be simplified by using Eqs. (1) to eliminate the cavity photon fields ϕ and write everything in terms of the exciton fields ψ. It is also convenient to approximate $\omega_x^2-\omega_p^2\approx 2\omega_x(\omega_x-\omega_p)$, etc., and define $\Omega=g/\omega_x$, $\bar{\kappa}=\frac{1}{2}\kappa/\omega_x$, and $f=\frac{1}{2}F/\omega_x$. Then Eqs. (2) become

$$
\left(\omega_x+\bar{\kappa}|\psi_p|^2-\omega_p-\frac{(\Omega/2)^2}{\omega_c(k_p)-\omega_p}\right)\psi_p+2\bar{\kappa}\psi_s\psi_i\psi_p^*
=\tfrac{1}{2}\Omega f_p/[\omega_c(k_p)-\omega_p], \qquad (3a)
$$

$$
\left(\omega_x+2\bar{\kappa}|\psi_p|^2-\omega_s-\frac{(\Omega/2)^2}{\omega_c(k_s)-\omega_s}\right)\psi_s+\bar{\kappa}\psi_p^2\psi_i^*
=\tfrac{1}{2}\Omega f_s/[\omega_c(k_s)-\omega_s], \qquad (3b)
$$

$$
\left(\omega_x+2\bar{\kappa}|\psi_p|^2-\omega_i-\frac{(\Omega/2)^2}{\omega_c(k_i)-\omega_i}\right)\psi_i+\bar{\kappa}\psi_p^2\psi_s^*=0. \qquad (3c)
$$

Equations (3) constitute the basic model for parametric processes in a microcavity. The terms in $|\psi_p|^2$ represent the renormalization of the exciton energy due to the pump population. The other nonlinear terms provide the scattering, which is the main interest here: $\bar{\kappa}\psi_p^2\psi_i^*$ and $\bar{\kappa}\psi_p^2\psi_s^*$ in Eqs. (3b) and (3c) describe the buildup of the population in the signal and idler modes, while $2\bar{\kappa}\psi_s\psi_i\psi_p^*$ in Eq. (3a) represents the corresponding pump depletion.

It is often useful to make the simplification of considering a situation where the pump, signal, and idler energies are all close to the corresponding polariton resonance values, and the broadenings are small compared to the Rabi splitting Ω. Then it is a good approximation to replace the polariton response by a single Lorentzian function at each **k**, with strength $|X|^2$, where X is the exciton amplitude (Hopfield coefficient) for the mode. The driving terms on the right-hand side of Eqs. (3) can similarly be approximated by $(C/X)f$, where C is the photon amplitude. Then, Eqs. (3) reduce to

$$
|X_p|^{-2}(\omega_p^0+i\gamma_p-\omega_p)\psi_p+2\bar{\kappa}\psi_s\psi_i\psi_p^*=(C_p/X_p)f_p, \qquad (4a)
$$

$$
|X_s|^{-2}(\omega_s^0+i\gamma_s-\omega_s)\psi_s+\bar{\kappa}\psi_p^2\psi_i^*=(C_s/X_s)f_s, \qquad (4b)
$$

$$
|X_i|^{-2}(\omega_i^0+i\gamma_i-\omega_i)\psi_i+\bar{\kappa}\psi_p^2\psi_s^*=0, \qquad (4c)
$$

where ω_p^0, ω_s^0, and ω_i^0 are the polariton resonance frequencies and γ_p, γ_s, and γ_i the corresponding widths. In writing the equations in this form, the exciton renormalization is effectively ignored, though it can be considered to be included as a renormalization of the polariton frequencies: at each point on the dispersion, it leads to a blueshift of approximately $2\bar{\kappa}|X|^2|\psi_p|^2$. For low pump powers, where the blueshift is small compared to the pump polariton width, and when $\omega_p=\omega_p^0$, ψ_p can be approximated, using Eq. (4a), by $\psi_p\approx -iC_pX_p^*f_p/\gamma_p$, and the blueshift is

$$
\delta\omega^0\approx 2\bar{\kappa}|X|^2(|C_p|^2|X_p|^2/\gamma_p^2)I_p, \qquad (5)
$$

where $I_p=|f_p|^2$ is the pump intensity.

It is interesting to compare the present classical model with the treatment in Ref. 3, which gives a good fit to the pump-probe parametric amplifier experiments of Ref. 1. This treatment was based on a quantum mechanical picture of the exciton-exciton scattering process. However, with the approximations that were made, Eqs. (1)–(3) of Ref. 3, contain essentially the same physics as Eqs. (4) here. Of course, using a microscopic model gives a value for the nonlinearity $\bar{\kappa}$. However, $\bar{\kappa}$ only imposes a scale on the problem: rescaling all the fields so $\psi\rightarrow\psi/\sqrt{\bar{\kappa}}$, $f\rightarrow f/\sqrt{\bar{\kappa}}$, effectively makes $\bar{\kappa}=1$.

II. PARAMETRIC AMPLIFIER

In the parametric amplifier, both f_p and f_s are nonzero. It is also helpful to assume that $f_s \ll f_p$, so that ψ_s and ψ_i are small, and the pump depletion term in Eqs. (3a) and (4a) can be neglected. Consider first the situation when the probe, idler, and pump satisfy the triple resonance condition, so Eqs. (4) can be used with $\omega_p = \omega_p^0$, $\omega_s = \omega_s^0$, and $\omega_i = \omega_i^0$. Without the pump depletion term, these equations are solved by eliminating ψ_p and ψ_i using Eq. (4a) and then Eq. (4c), to get

$$\psi_s = \frac{-iC_s X_s^* f_s/\gamma_s}{1-\overline{\kappa^2}(|X_i|^2|X_s|^2/\gamma_i\gamma_s)(|C_p|^4|X_p|^4/\gamma_p^4)|f_p|^4}. \quad (6)$$

Dividing by the value of ψ_s without the pump, i.e., with $f_p = 0$, gives the *internal gain* for the probe:

$$\alpha_s = 1/(1-I_p^2/I_0^2), \quad (7)$$

where

$$I_0 = \gamma_p^2\sqrt{\gamma_s\gamma_i}/(\overline{\kappa}|C_p|^2|X_p|^2|X_s||X_i|). \quad (8)$$

The gain increases from unity at $I_p = 0$ to become singular at $I_p = I_0$. This suggests that I_0 represents the threshold pump intensity for oscillation, which will indeed be shown to be the case in the next section.

The previous discussion was limited to the case where all the fields are on resonance. If this condition is not satisfied, it is still possible to obtain an analytic solution when the exciton renormalization is neglected. Solving Eqs. (3) with the same weak probe approximation gives

$$\psi_s = \frac{-(\Omega/2)f_s/\Lambda_s}{1-\overline{\kappa^2}[(\omega_c(k_s)-\omega_s)/\Lambda_s][(\omega_c(k_i)^*-\omega_i)/\Lambda_i^*][(\Omega/2)^4/|\Lambda_p|^4]|f_p|^4}, \quad (9)$$

where $\Lambda_p = (\omega_x - \omega_p)[\omega_c(k_p) - \omega_p] - (\Omega/2)^2$, and Λ_s and Λ_i are similarly defined.

Figure 1 shows the signal response at normal incidence, calculated using Eq. (9), for different pump angles. The pump energy is varied to be on the polariton resonance for each angle. The spectra show the two polariton features at normal incidence, with clear gain on the lower branch for pump angles in the region of 16°: for this pump angle, the pair scattering resonance condition is satisfied when the probe angle is 0°.

In Fig. 2, the signal response is mapped out as a function of energy and angle with the pump kept on resonance at 16°. There is an enhanced probe response when either the signal or the idler is on resonance—these single resonance energies are indicated by the dashed lines on the figure. The response is much stronger for the signal resonance, because the probe couples to the signal directly, but to the idler only via parametric scattering. The strongest response occurs at the double resonances, where the dashed lines intersect (at 0°, 16°, and 33.5°), but there is a long segment of the dispersion very close to double resonance, where the gain remains high.

III. PARAMETRIC OSCILLATOR

In the parametric oscillator regime, there is no probe, so $f_s = 0$, but solutions can still be found with finite signal and idler fields. Again, it is simplest to start with the triply resonant case. Focusing on Eqs. (4b) and (4c), taking the complex conjugate of one of them, and treating ψ_p as a parameter, we see that there are nonzero solutions for ψ_s and ψ_i only if the determinant of the coefficients is zero, that is,

$$\overline{\kappa}|\psi_p|^2|X_s||X_i| = \sqrt{\gamma_s\gamma_i}. \quad (10)$$

The physical interpretation of this condition is obvious—for a steady state solution, the generation rate of polaritons in the signal and idler directions, on the left-hand side, must equal the (geometric) mean of the loss rates, $\sqrt{\gamma_s\gamma_i}$. This is only possible with the value of ψ_p in Eq. (10). For a given external driving field f_p, the required value of ψ_p is attained by the depletion of the pump polariton field due to the stimulated scattering term.

The resulting signal intensity is calculated by using Eq. (4b) to write ψ_i in terms of ψ_s, then substituting in Eq. (4a) to obtain

$$|\psi_s|^2 = \frac{\gamma_i}{2\overline{\kappa^2}|\psi_p|^3|X_i|^2}\frac{|C_p|}{|X_p|}\left(|f_p| - \frac{|\psi_p|}{|C_p||X_p|}\gamma_p\right), \quad (11)$$

where $|\psi_p|$ is now just a constant given by Eq. (10). Since the emitted signal intensity I_s is proportional to $|\psi_s|^2$, this relationship is of the form

$$I_s \propto \sqrt{I_p} - \sqrt{I_0}, \quad (12)$$

where I_0 is the same threshold intensity as in Eq. (8). Of course $I_s \geq 0$, so this solution only exists when $I_p \geq I_0$.

The treatment can be extended to the case where the signal direction is such that the signal and idler are not both on resonance, that is, the mismatch $\Delta = 2\omega_p - \omega_s^0 - \omega_i^0 \neq 0$. The steady state condition, Eq. (10), becomes

$$\overline{\kappa}|\psi_p|^2|X_s||X_i| = [(\omega_s^0 + i\gamma_s - \omega_s)(\omega_i^0 - i\gamma_i - \omega_i)]^{1/2}, \quad (13)$$

with, once again, $\omega_i = 2\omega_p - \omega_s$. A solution is only possible if the right-hand side of Eq. (13) is real, which requires $\omega_s - \omega_s^0 = \Delta\gamma_s/(\gamma_s+\gamma_i)$, and correspondingly $\omega_i - \omega_i^0 = \Delta\gamma_i/(\gamma_s+\gamma_i)$. The physical significance of this requirement can be seen by looking at ψ_s and ψ_i: for the allowed value of ω_s, $\gamma_s|\psi_s|^2/|X_s|^2 = \gamma_i|\psi_i|^2/|X_i|^2$, that is, the loss rates through the signal and idler modes are identical. Hence

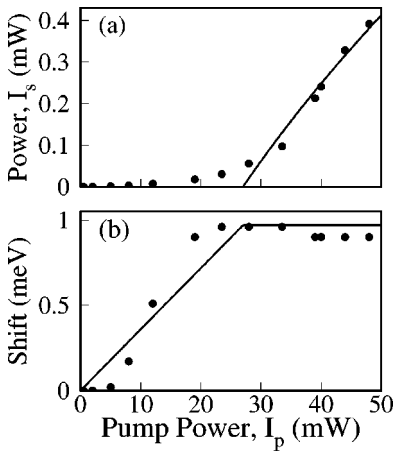

FIG. 3. Theoretical fits to the experimental data (points) for (a) signal power and (b) blueshift from Ref. 5.

this is the Manley-Rowe condition for the microcavity parametric oscillator.

Continuing the solution for the signal intensity, for resonant pumping the effect of the finite mismatch Δ is to shift the threshold, so

$$I_0(\Delta) = I_0(0)\{1+\Delta^2/(\gamma_s+\gamma_i)^2\}^{1/2}, \tag{14}$$

where $I_0(0)$ is the value given in Eq. (8). The threshold is lowest when $\Delta=0$ and pump, signal, and idler are all on resonance.

These results show that the signal intensity is determined by the pump depletion, which produces the value of $|\psi_p|^2$ required by Eqs. (10) and (13). For $I_p > I_0$, $|\psi_p|^2$ remains unchanged, just as the population inversion in a conventional laser is clamped at its threshold level. Since the actual value of $|\psi_p|^2$ is unique to a particular pair of signal and idler directions, in equilibrium there can only be one finite signal amplitude. It is easy to see what will happen in an out-of-equilibrium situation when there is more than one signal. A signal whose loss rate exceeds its generation rate will decay, while one for which the generation rate exceeds the loss will grow. So, in a process akin to mode selection in a laser, the signal with the lowest loss rate will dominate, depleting the pump until only it survives.

IV. DISCUSSION

This model of the parametric oscillator makes two simple predictions that can be checked against experiment: the $\sqrt{I_p}$ power dependence in Eq. (12), and the clamping of the pump polariton amplitude ψ_p to the value given in Eq. (10). The latter effect should be observable as a saturation, above threshold, of the blueshift of the polariton dispersion. Below the threshold the shift is roughly linear with pump power, and it saturates at the value given in Eq. (5) with $I_p = I_0$. For the signal mode the saturated shift is thus $\delta\omega_s^0 \approx 2\sqrt{\gamma_s\gamma_i}|X_s|/|X_i|$. Of course, there are other effects, not included in the model, that can cause energy shifts. These include the exciton renormalization due to the signal field and at higher powers the breakdown of the strong-coupling regime. The former effect can be estimated and is small: the signal field will give an energy shift of $\overline{\kappa}|X_s|^2|\psi_s|^2$, which is about 10% of the saturated $\delta\omega_s^0$ when $I_p = 2I_0$, using the same structural parameters as in Fig. 1.

Figure 3 shows how these predictions compare with the experimental results in Ref. 5. The signal power is fitted to the form $I_s \propto \sqrt{I_p} - \sqrt{I_0}$ of Eq. (12). Although a good fit is obtained, it is difficult to distinguish the $\sqrt{I_p}$ behavior from a simple linear increase with the limited range of data above threshold. The support for the model provided by the blueshift data is rather better: the experiments show a clear saturation of the blueshift, and the saturation shift of just under 1 meV agrees very well with the prediction of $\delta\omega_s^0 \approx 0.97$ meV obtained using the experimental widths $\gamma_s = 0.57$ meV and $\gamma_i = 0.80$ meV.

The predicted form of the gain in Eq. (7) is not found in the pump-probe experiments of Ref. 1, where the gain increases exponentially with I_p. However, the gain mechanism in the ultrafast measurements differs from the cw parametric amplification discussed here. The peak pump powers in the experiments are orders of magnitude greater than the threshold I_0, but oscillator behavior is not seen because there is insufficient time for the signal to build up just from the incoherent photoluminescence. However, the probe pulse seeds the signal, starting an an exponential growth that lasts as long as the pump. This gives the observed exponential dependence on I_p. Although the cw gain below threshold predicted here has not been seen experimentally, it should be observable in structures that show parametric oscillator behavior.

To conclude, it has been shown that the parametric oscillator behavior recently observed in microcavities can be well explained by a simple classical treatment of a nonlinear exciton strongly coupled to a cavity mode. The main nonclassical effects that are missing from this model are the incoherent photoluminescence, discussed theoretically in a recent paper by Ciuti *et al.*,[8] and quantum statistical effects in the oscillator behavior around the threshold. It is also possible that at higher excitation powers the signal intensity will become large enough for the appearance of new physics due to polariton-polariton interactions in the coherent state.

I gratefully acknowledge the contributions made by P. B. Littlewood, M. S. Skolnick, J. J. Baumberg, P. G. Saviddis, and R. M. Stevenson in discussions about this work.

[1] P.G. Savvidis *et al.*, Phys. Rev. Lett. **84**, 1547 (2000).
[2] R. Huang *et al.*, Phys. Rev. B **61**, R7854 (2000).
[3] C. Ciuti *et al.*, Phys. Rev. B **62**, R4825 (2000).
[4] R.M. Stevenson *et al.*, Phys. Rev. Lett. **85**, 3680 (2000).
[5] J.J. Baumberg *et al.*, Phys. Rev. B **62**, R16 247 (2000).
[6] R. Houdré *et al.*, Phys. Rev. Lett. **85**, 2793 (2000).
[7] See, for example, Y. R. Shen, *The Principles of Nonlinear Optics* (Wiley, New York, 1984), Chap. 9.
[8] C. Ciuti *et al.*, Phys. Rev. B **63**, R041303 (2001).